Structure of ^{20}Ne states in resonance ^{16}O+α elastic scattering

D. K. Nauruzbayev, V. Z. Goldberg, A. K. Nurmukhanbetova, M. S. Golovkov, A. Volya, G. V. Rogachev, and R. E. Tribble

Phys. Rev. C **96**, 014322 — Published 28 July 2017

DOI: 10.1103/PhysRevC.96.014322

Structure of ^{20}Ne states in the resonance ^{16}O+α elastic scattering

D. K. Nauruzbayev,[1,2,*] V. Z. Goldberg,[3] A. K. Nurmukhanbetova,[1,†]
M. S. Golovkov,[4,5] A. Volya,[6] G. V. Rogachev,[3] and R. E. Tribble[3]

[1] *National Laboratory Astana, Nazarbayev University, Astana, 010000, Kazakhstan*
[2] *Saint Petersburg State University, Saint Petersburg, 199034, Russia*
[3] *Cyclotron Institute, Texas A&M University, College station, Texas, 3366, USA*
[4] *Joint Institute for Nuclear Research, Dubna, 141980 , Russia*
[5] *Dubna State University, Dubna, 141980, Russia*
[6] *Department of Physics, Florida State University, Tallahassee, Florida, 32306, USA*

Background: The nuclear structure of the cluster bands in ^{20}Ne presents a challenge for many theoretical approaches. It is especially difficult to explain the broad 0^+ and 2^+ states, both at around 9 MeV excitation energy. More reliable experimental data for these levels is important for proper quantitative assessment and development of theoretical methods.

Purpose: To obtain new data on ^{20}Ne α-cluster structure.

Method: Thick target inverse kinematics technique was used to study the ^{16}O+α resonance elastic scattering and the data were analyzed using an R-matrix approach. The ^{20}Ne spectrum, the cluster and nucleon spectroscopic factors were calculated using cluster-nucleon configuration interaction model (CNCIM).

Results: We determined the parameters of the broad resonances in ^{20}Ne: 0^+ level at 8.77 ± 0.150 MeV with a width of 750^{+500}_{-220} keV; 2^+ level at 8.75 ± 0.100 MeV with the width of 695 ± 120 keV; the width of 9.48 MeV level of 65 ± 20 keV; and showed that 9.19 MeV, 2^+ level (if exists) should have width ≤ 10 keV. A detailed comparison of the theoretical CNCIM predictions with the experimental data on cluster states was made.

Conclusions: Our experimental results obtained by the TTIK method generally confirm the adopted data on α cluster levels in ^{20}Ne. The CNCIM gives a good description of the ^{20}Ne positive parity states up to an excitation energy of ~ 7 MeV, predicting reasonably well the excitation energy of the states and their cluster and single particle properties. At higher excitations, a qualitative disagreement with the experimentally observed structure is evident, especially for broad resonances.

I. INTRODUCTION

It is well recognized that the α particle interaction with atomic nuclei is important in astrophysics [1]. Even if astrophysical reactions involving helium do not proceed through the strong α-cluster states (because of their high excitation energy), these states can provide α width to the states that are closer to the region of astrophysical interest through configuration mixing.

For a long time, the surprising alpha cluster structure has been a stimulus for the development of classical shell model approaches (see [2] for new results). Additionally, recent work by the authors of Ref. [3] "strengthened the theoretical motivation for experimental searches of alpha cluster states in alpha-like nuclei". The authors of Ref. [3] relate the nuclear structure in light even-even systems with equal number of protons and neutrons with the first-order phase transition at zero temperature from a Bose-condensed gas of alpha particles (^{4}He nuclei) to a nuclear liquid.

^{20}Ne nucleus is a classic example of the manifestation of the alpha-cluster structure, which makes it a touchstone for *ab initio* approaches [4]. The nucleus ^{20}Ne is a benchmark case for the traditional shell model and its extension into algebraic and clustering domains. The well-established effective interaction Hamiltonians such as [5] not only shows an outstanding agreement with experimental data for *sd*-shell nuclei but also generates configuration mixing that shows transition to deformation and clustering.

It is remarkable that almost all of the observed states below 10 MeV can be classified into several overlapping rotational-like bands. The ground state band (based on 0^+_1) has a transient character from the shell to the cluster structure; this stems from algebraic symmetry properties [2]. Three other bands based on 0^+ levels, on 0^+_2 at 6.72 MeV, on a very narrow 0^+_3 at 7.19 MeV, on a very broad 0^+_4 at ~ 8.7 MeV [6], are of evident cluster structure. The 0^+_2 and 0^+_4 bands have ^{16}O+α core structure as can be seen from their reduced α particle widths; probably the 0^+_3 band has a predominant ^{12}C+^{8}Be structure which manifests itself through the selectivity of the ^{8}Be transfer reactions [7]. The ground state band and the 0^+_2 band in ^{20}Ne can be related to similar structures in ^{16}O and ^{12}C, however the structure of "additional" 0^+_1 band-member states is not understood [4]. The cluster approaches [8] related the 0^+_4 band with the so-called "^{16}O + α" higher nodal band, which has one more node in the "^{16}O + α" relative wave function than the lower bands have. However, it appears that there are too many bands with a similar structure.

The α particle decay threshold in ^{20}Ne is 4.73 MeV, while the threshold for proton decay is at 12.8 MeV (neu-

* dosbol.ndk@gmail.com
† anurmukhanbetova@nu.edu.kz

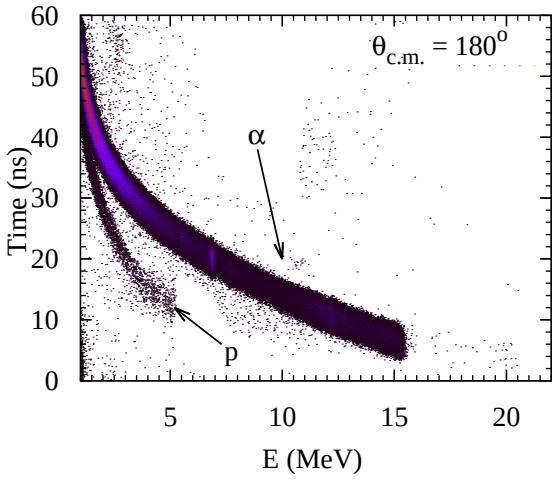

FIG. 1. E-T spectrum for the zero-degree detector. Alpha particles dominate; one can see also a weaker proton locus below the alpha particles.

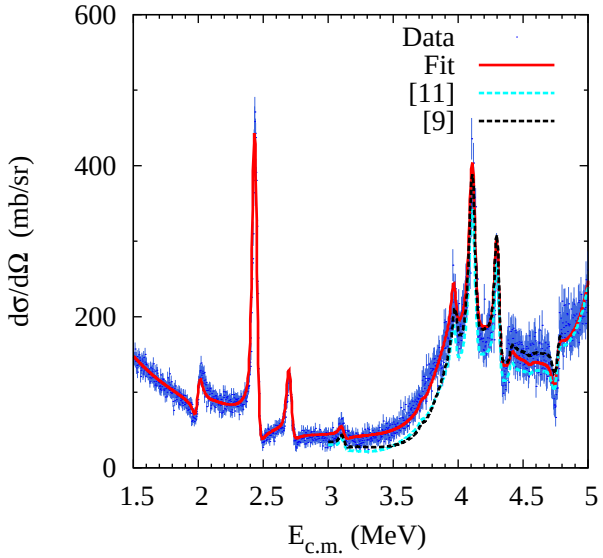

FIG. 2. The ^{16}O(α,α)^{16}O elastic scattering excitation function at 180°c.m. The excitation energies in ^{20}Ne, E_x in Table I, are related with c.m. energy, $E_{c.m.}$, by expression, $E_x = E_{c.m.} + 4.73$ MeV. The bold (red) line is the R-matrix fit with the parameters of the present work. The dotted (cyan) line is a fit with the 0^+_4 excitation energy being 8.3 MeV [11], and dotted (black) line is a fit where the 0^+_4 excitation energy is 8.62 MeV and the width is 1.472 MeV, Ref. [9].

tron decay threshold is even higher). Therefore, resonant α particle scattering is an evident way to obtain data on the natural parity levels in ^{20}Ne up to 13 MeV excitation energy. Indeed, in this energy region the majority of adopted data on level properties [6] is based on resonance scattering work of 1960s. More recently the $\alpha + ^{16}$O resonance scattering experiments were further improved to include backward angles and the resulting data were analyzed using R-matrix code Multi 6 [9]. The authors of Ref. [9] obtained quite different results from those used in Ref. [6] for many levels (see Table I); in particular, the broad 0^+_4 and 2^+_4 levels appeared even broader. The authors of Ref. [9] noted difficulties of the R-matrix fit in the region $6 - 8$ MeV of excitation energies, which is mainly free from narrow resonances. Evidently strong alpha clustering states of over 1.0 MeV width influence a very broad excitation region (for instance, see [10]).

T. Fortune et al. [11, 12] were the first to realize the drastic contradiction between the observed single particle structure of the broad states and shell model predictions. The authors of Refs. [11, 12] also proposed the idea of mixing between different configurations to explain the effect. The same idea was used in [13]. The authors of Refs. [11, 12] reached their conclusion using old data for the 0^+_2 state along with some estimates for the properties of the broad states proposed in Ref. [14]. Later measurements [6] gave the width of 19 keV for the 6.72 MeV state, which is about 25% larger than that used in work [11].

From an experimental perspective, the aim of this work is to obtain new information on the structure of ^{20}Ne states, especially on the broad 0^+ and 2^+ states. Unlike other experimentalists, we used the Thick Target Inverse Kinematics method (TTIK) (see [15–19] and references therein) to study the excitation functions for the ^{16}O(α,α)^{16}O elastic scattering in the ^{20}Ne excitation region of $5.5 - 9.6$ MeV and in a broad angular interval. On the theoretical side, we also used multi configuration shell model calculations to understand the limits of this approach in the description of the cluster states.

II. EXPERIMENT

The experiment was performed at the DC-60 cyclotron (Astana) [17] which can accelerate heavy ions up to 1.9 MeV/nucleon of energy. While the TTIK method can't compete with a classical approach in terms of energy resolution, the possibility of observing excitation functions at and close to 180 degrees, where the resonance scattering dominates over the potential scattering, enables one to obtain more reliable information on the broad states. In the TTIK technique the inverse kinematics is used. The light recoils, α particles, are detected from a scattering event. These recoils emerge from the interaction with the beam ions and hit a Si detector array located at forward angles while the beam ions are stopped in the gas, as α particles have smaller energy losses than the scattered ions. The TTIK approach provides a continu-

ous excitation function as a result of the slowing down of the beam.

For the present experiment, the scattering chamber was filled with helium of 99.99% purity. The 30 MeV ^{16}O beam entered the scattering chamber through a thin entrance window made of 2.0 μm Ti foil. Eight monitor Si detectors were placed in the chamber to detect ^{16}O ions elastically scattered from the Ti foil at 21° angle. This array monitors the intensity of the beam with precision better than 4%. Fifteen 10×10 mm^2 Si detectors were placed at a distance of ~ 500 mm from the entrance window in the forward hemisphere at different laboratory angles starting from zero degrees. The gas pressure was chosen to stop the beam at distance of ~ 40 mm from the zero-degree detector. The detector energy calibration and resolution (~ 30 keV) were tested with a ^{226}Ra, ^{222}Rn, ^{218}Po, and ^{214}Po α-source. The experimental setup was similar to that used before [19], and more details can be found in Refs. [17, 19]. The main errors in the present experimental approach are related to the uncertainties of the beam energy loss in the gas. To test the energy loss, we placed a thin Ti foil (2.0 μm) at different distances from the entrance window. This can be used during the experiment without cycling vacuum. Our tests were consistent with the tabulated data [20] for energy loss of ^{16}O in helium. The details of these tests will be published elsewhere. As a result, we estimated that the uncertainties in the absolute cross section are less than 6%. This conclusion was tested by comparison with the Rutherford cross sections at low energies. At all angles the agreement with the Rutherford scattering cross section is within 5% (see Fig. 3).

Together with the amplitude signal, the Si detectors provided for a fast signal. This signal together with a "start" signal from RF of the cyclotron was used for the Time-of-Flight (TF) measurements. This E-T (Energy-Time) combination is used for particle identification in the TTIK approach [16–18]. Of course, only α particles should be detected as a result of the interaction of ^{16}O with helium at the chosen conditions. However, protons can be created in the Ti window, and protons can appear due to hydrogen admixtures in the gas. Indeed, we have observed a weak proton "banana" on the E-T plot, likely as a result of reactions in the window. These protons were easily identified by TF and separated from the α particles, as seen in Fig. 1.

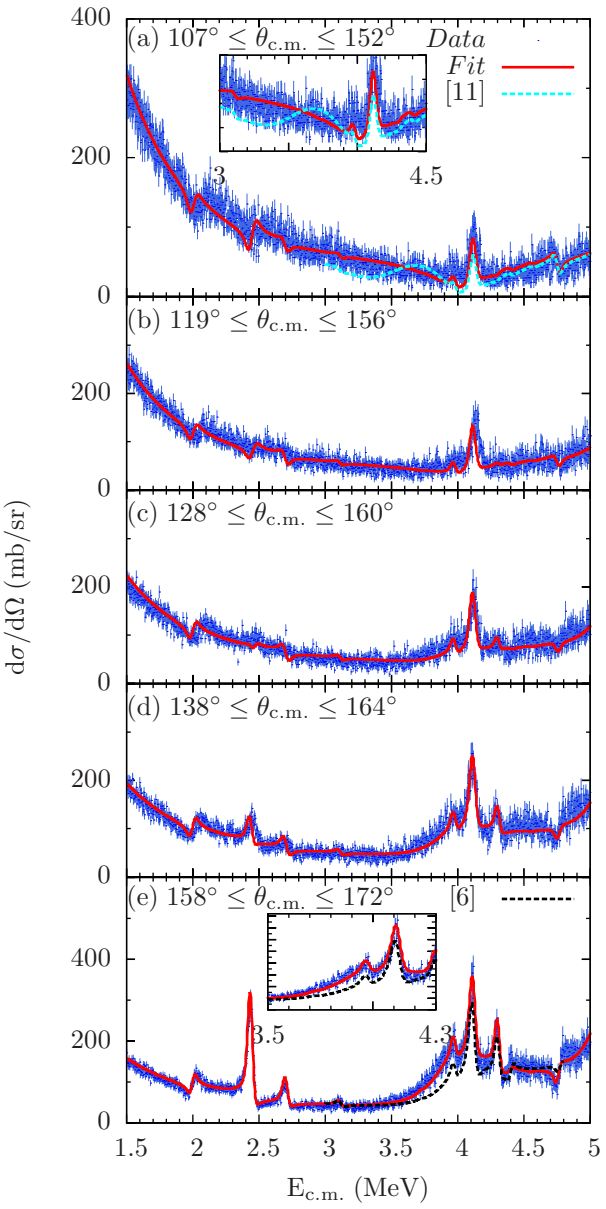

FIG. 3. R-matrix fit (bold red curve) of the excitation functions for the α+^{16}O elastic scattering. (a) The dashed (cyan) curve presents the fit when the 0_4^+ level is placed at the 8.3 MeV excitation energy [11] and (e) dotted (black) line is a fit with 2^+ level at the excitation energy of 9.0 MeV [6].

III. EXPERIMENTAL RESULTS AND DISCUSSION

The experimental excitation functions were analyzed using multilevel multichannel R-matrix code [21]. The calculated curves were convoluted with the experimental energy resolution. The experimental energy resolution was $\sim$ 30 keV at zero degrees and deteriorated up to $\sim$ 90 keV with angles diverging from zero degrees. We did not notice a deterioration of the energy resolution with the energy loss of the beam in the chamber. As seen in Table I, the excitation energies of the resonances of the present work agree with the adopted ones [6] within $10 - 15$ keV. This agreement confirms good overall energy calibration and the correct account of the ion energy loss in helium in our work. Fig. 2 and Fig. 3 show the experimental excitation functions together with the present R-matrix fit. Fig. 2 displays the data at 180° c.m. angle and illustrates the differences in the fits due to different parameters of the broad 0_4^+ resonance. The data on the

TABLE I. ^{20}Ne levels

Level	TUNL data [6]			H. Shen et al. [9]		This work			CNCIM			
	E_x (MeV)	J^π	Γ_α (keV)	E_x (MeV)	Γ_α (keV)	E_x (MeV)	Γ_α (keV)	γ_α	E_x (MeV)	J^π	SF_p	SF_α
1	0	0_1^+		-	-	0		Large	0	0^+	0.36	0.73
2	1.63	2_1^+		-	-	1.63		Large	2.242	2^+	0.41	0.67
3	4.25	4_1^+		-	-	4.25		Large	4.58	4^+		0.62
4	5.79	1^-	$(28 \pm 3) \times 10^{-3}$	-	-	4.45	0.03	1.4				
5	6.72	0_2^+	19 ± 0.9	6.72	11	6.78	20.6	0.47	6.94	0_3^+	0.55	0.46
6	7.16	3^-	8.2 ± 0.3	7.16	10	7.18	8.3	1.37				
7	7.19	0_3^+	3.4 ± 0.2	7.19	5	7.20	3	0.019	6.27**	0_2^+	0.055	0.44**
8	7.42	2_2^+	15.1 ± 0.7	7.43	7	7.44	14.3	0.19	7.39	2_3^+	0.01	0.12
9	7.83	2_3^+	2	7.83	1	7.85	3.68	0.01	7.15**	2_2^+	0.12	0.18**
10	8.45	5^-	0.013 ± 0.004	8.45	0.02	8.45	0.013					
11	8.71	1^-	2.1 ± 0.8			8.71	3.5					
12	≈ 8.7	0_4^+	> 800	8.62	1470	8.77 ± 0.15	750^{+500}_{-220}	~ 0.25	9.66**	0_4^+	0.002	0.18**
13	8.78	6_1^+	0.11 ± 0.02	-	-	8.78	0.14	0.5	9.49	6^+		0.51
14	8.85	1^-	19	8.84	27	8.85	18.0					
15	9.00	2_4^+	≈ 800	8.87	1250	8.79 ± 0.10	695 ± 120	0.86	8.36**	2_4^+	0.02	0.02**
16	9.03	4_3^+	3	9.02		9.03	1.9	0.03	9.0	4^+		0.09
17	9.12	3^-	3.2	9.09	4	9.13	4.1					
18	9.19	2^+		-	-	(9.29)	≤ 10					
19	9.48	2^+	29 ± 15	9.48	46	9.48	65 ± 20	0.02				
20	9.99	4_4^+	155 ± 30	10.02	150	9.97	157	0.38	9.5	4^+		0.009
21*	10.26	5^-	145 ± 40	10.26	190	10.26		1.9				
22	10.41	3^-	80	10.40	101	10.41						
23	10.58	2^+	24	10.56	15	10.58			10.2	2+	0.005	0.04
24	10.80	4_4^+	350	10.75	400	10.80			10.7	4^+		0.04
25	10.97	0_5^+	580	10.99	700	10.97			11.9	0^+		
26	11.24	1^-	175	11.19	85	11.24						
27	11.95	8^+	$(3.5 \pm 1.0) \times 10^{-2}$			11.95		0.35	11.50	8^+		0.40

*For the levels with numbers 21-27 the parameters of the present fit were fixed as in Ref. [6]
**Calculated in *psd* space SF is to the first excited state in ^{16}O; SFs for the ground state in ^{16}O are ≤ 0.1

resonances used in the present R-matrix fit are summarized in Table I together with the adopted data [6]. Data of the last R-matrix analysis [9] are also given in Table I. The analysis [9] resulted in level parameters which are often different from the adopted ones.

In the detailed description of the narrow states (widths less than 10 keV) our analysis (Table I) resulted in small discrepancies with the data in Ref. [6]. The small disagreements for the narrow states are not significant because in order to accelerate automatic fit calculations the R-matrix code [21] is tuned for the TTIK measurements and for the analyses of states with a width of over 10 keV. Here we focus on the broader states and on the part of the excitation function changing slowly with energy and angle.

Our analysis indicates that all strong alpha cluster states at $5 \sim 6$ MeV below or above the investigated excitation energy region can influence the R-matrix fit. Therefore, we included the ^{20}Ne ground state, the first 0^+, 2^+, 4^+ states and 1^- (5.79 MeV) state (see Table I) in the fit, even though they are below the investigated region. Among these states, only the 1^- state is above the α particle decay threshold in ^{20}Ne; the reduced width of this state is known, and it is large. Shell model calculations, discussed in what follows, also give large spectroscopic factors for all members of the ground state band. Our results support this since for good agreement in observed excitation functions one needs large values of the corresponding amplitudes (over 0.7). Above the investigated excitation energy region, there are known high spin α-cluster resonances. Each of these resonances (see Table I) considered separately has a noticeable influence on the fit, especially at 180°. However, their combined influence is much weaker. This cancellation is due to complex interference of states with different parities and spins. Only the influence of the closest to the investigated region, the 4^+ (9.99 MeV) resonance is noticeable. A somewhat better fit needs the width of this resonance to be slightly larger ~ 160 keV (well within the quoted uncertainties, see Table I). Parameters of all other resonances above the investigated region were fixed according to the data of Ref. [6]. A good general fit ($\chi^2 = 1.1$) was reached in this way without any backward resonance inclusion.

TABLE II. $\alpha + {}^{12}$C levels in ^{16}O

^{16}O level	$\Gamma_{\alpha\ \mathrm{exp}}$ keV [6]	$\gamma_\alpha(1)$; -V$_0$ MeV	$\gamma_\alpha(2)$; -V$_0$ MeV	$\gamma_\alpha(3)$; -V$_0$ MeV
1^-, 9.58 MeV	420 ± 20	0.70; 138.2	0.72; 150.0	0.84; 158.5
4^+, 10.36 MeV	26 ± 3	0.68; 125.3	0.88; 139,6	1.21; 143.2

All resonances are at the maximum at 180° c.m. The broad hump at this angle and c.m. energy of 4 MeV (Fig. 2) is a clear indication for the presence of low spin states, 0^+ and 2^+. Higher spin states are narrower. A single level (2^+) cannot produce the strong peak at different angles, and levels of different parity, such as 2^+ and 1^-, interfere destructively at 180°. The present analysis resulted in two practically degenerate states at ~ 8.8 MeV with the same width (see Table I). Our results for the broad 2^+ are rather close to the adopted values. However, if this level is moved to 9.0 MeV excitation energy (as in Ref. [6]) then the fit becomes worse, especially in the vicinity of the dip due to the presence of another 2^+ level at 9.48 MeV (Fig. 3(e)). The fit becomes even worse if a very broad 2^+ level that follows from the parameters of Ref. [9] is considered.

In their study of ^{20}Ne, T. Fortune at al., [11] observed a broad distribution with a center at 8.3 MeV excitation energy and related it to the 0_4^+ resonance. Fig. 2 presents the R-matrix excitation function where the 0_4^+ level is placed at 8.3 MeV excitation energy. This move destroys the good fit. Fig. 2 shows that a very broad 0^+ level from the fit in Ref. [9] also destroys the agreement.

The 18^{th} (2^+) level of Ref. [6] is in the energy region of the present investigation. It was observed in a single work in a study of ^{20}Na β^+ decay. We have not found any reliable evidence for the presence of this state. If it exists, its width should be less than 10 keV. We observe a fluctuation of points which might be associated with a narrow 2^+ level at excitation energy of 9.29 MeV.

We note that the 19^{th} level, 2^+, was found in our fit to have the adopted [6] excitation energy but a different width of 65 ± 20 keV. While the factor of two difference in the widths as compared to Ref. [6] marginally exceeds the error bars, the better resulting fit is evident. For this state the adopted data in Ref. [6] are based on the results of a single older work [22]. The authors of Ref. [22] observed a weak γ decay of this state in the presence of a large background. A broader level than in Ref. [22] was also found in work [9] as shown in Table I.

We characterize the alpha-cluster properties of the states above the alpha particle decay threshold by SF $= \gamma_\alpha = \Gamma_{\alpha\ \mathrm{exp}}/\Gamma_{\alpha\ \mathrm{cal}}$, where $\Gamma_{\alpha\ \mathrm{cal}}$ is the single alpha particle width calculated in the α-core potential. To calibrate the potential the SFs were first calculated for the well-known alpha-cluster states in ^{16}O.

The Woods-Saxon potential was used to calculate the limit ($\Gamma_{\alpha\ \mathrm{cal}}$) for the width of the single particle states. First we fit the widths of known alpha-cluster states, 1^- and 4^+, in ^{16}O so that $\gamma_\alpha = \Gamma_{\alpha\ \mathrm{exp}}/\Gamma_{\alpha\ \mathrm{cal}} \sim 1.0$. The real part of the potential was changed to fit the binding energy of the states. The radius of the potential was chosen to be R = r$_0$ $\times 12^{1/3}$; the Coulomb potential was taken into account as a charge sphere potential with R$_{\mathrm{coul}}$ = R. We made our first calculations (1) with r$_0$ = 1.31 fm and the diffuseness a = 0.65 fm, then we set r$_0$ = 1.23 fm (2), and we finally performed a third set of calculations (3) with r$_0$ = 1.23 fm and a = 0.6 fm. The results are summarized in Table II. The γ_α calculations for the ^{20}Ne states are made with the final (third, 3) set of parameters, because these parameters provide for a better description of the widths of the known ^{16}O alpha cluster states. In the following section, these γ_α are compared with SFs obtained theoretically.

IV. THEORETICAL DESCRIPTION OF THE α-CLUSTER STATES IN ^{20}Ne

The CNCIM [2] is among the latest developments of the classical shell model approaches towards clustering. This model targets a combination of configuration interaction techniques with algebraic methods that emerge in the description of clustering. The ability to construct a fully normalized set of orthogonal cluster channels is at the core of this approach; the overlaps of the shell model states with these channels are associated with spectroscopic factors and compared in Table I with the reduced widths. The CNCIM allows us to study clustering features that emerge in models with well-established traditional shell model Hamiltonians. These effective model Hamiltonians are built from fundamental nucleon-nucleon interactions followed by phenomenological adjustments to select observables; thus, they generally describe a broad scope of experimental data with high accuracy. Apart from using these phenomenological shell model Hamiltonians, our study does not involve any adjustable parameters. In order to fully explore the problem, we considered several different model spaces and corresponding Hamiltonians: the *sd* model space with USDB interaction [5]; unrestricted *p-sd* shell model Hamiltonian [23], the same Hamiltonian has been used in Ref. [2]; WBP Hamiltonian [24] allowing $0\hbar\omega$, $1\hbar\omega$, and $2\hbar\omega$ excitations in *p-sd-pf* valence space; and the *sd-pf* Hamiltonian [25]. This sequence of Hamiltonians represents and expands the valence space from *sd* to *p-sd*, to *p-sd-pf*. All models are in good agreement for the *sd*-states; the low-lying negative parity states as well as positive $2ph$ excitations are dominated by the *p-sd* configurations. Thus, in Table I we only include the results from the *p-sd* Hamiltonian which turned out to be most representative. However, the following discussion

and conclusions are largely based on comparisons. The lowest states associated with significant *fp* shell component appear at excitation energies above 15 MeV.

Shell model calculations for ^{20}Ne with open *1s-0d (sd)* shells predict the ground state band well. The structure of this band is based on the dominating SU(3) configuration (about 75%) with quantum numbers (8,0). The model predicts (Table I) large SF for all members of the band based on the ground state in ^{20}Ne. The 0^+, 2^+, and 4^+ members of the band are below the α particle decay threshold and do not have observable α particle widths. However, large α cluster SFs for these states provide for a better R-matrix fit. While uncertainties for the R-matrix amplitudes for these states are large, the fit (Fig. 2 and 3) requires these amplitudes to be close to those of the negative parity states with the known extreme α cluster structure. The α particle widths of the highest 6^+ and 8^+ members of this band are known. There is a long history of attempts and ideas to describe these widths using shell model approaches (see, for instance Ref. [5]). Most calculations predicted large clustering for the band but could not explain the decrease of the reduced width for the 6^+ and 8^+ members. As one sees in Table I, the CNCIM calculations are in fine agreement with the experimental data for these states. All members of this band have significant clustering that diminishes at higher energies due to configuration mixing. The second 0^+ state within *sd* space appears at around 6.7 MeV of excitation (in *psd* model in Table I, this is a third 0^+ state at 6.9 MeV). This state also has a substantial clustering component and absorbs nearly all 15% of the remaining strength of the SU(3) (8,0) component. The following 2_2^+ (in experiment and in *sd* model, but third in *p-sd* model as discussed in what follows) at about 7.4 MeV of excitation energy being a member of the 0_2^+ band can be described in a similar way.

A defrost of the *0p* shell (which is filled in ^{16}O) results in the doubling of the levels, the new levels 0^+ and 2^+ appear. This is observed and shown in Table I, as marked with asterisks. In our calculations, the ordering in energy is reversed for both doublets. Structurally, the members of each doublet are very different. This allows them to be so close in energy while inhibiting configuration mixing and Wigner level-repulsion. One of the levels in each doublet (the lower 0^+ and lower 2^+) has a large α cluster SF relative to the first excited state in ^{16}O and much smaller SF relative to the ground state in ^{16}O (note that the theory gives the wrong order for the levels in question, see Table I). Indeed, the predicted difference in the structure is supported by population selectivity in different nuclear reactions. The 6.72 MeV 0^+ and 7.42 MeV 2^+ are populated much stronger than the neighboring 7.19 and 7.83 MeV levels in the ^{16}O(^{6}Li,d) reaction [26]. The opposite is the case in the ^{12}C(^{9}Be,n) or ^{12}C(^{12}C,α) reactions [27].

The theory gives large single particle spectroscopic factors for the *sd* states and smaller for the 7.19 and 7.83 MeV states. Indeed, one expects that states in ^{20}Ne with a hole in the p shell will be weakly excited in the single nucleon transfer, ^{19}F(^{3}He,d) reaction, in accordance with the experimental data [28]. The experiments [11, 12, 28] also support detailed single particle SF results from the same theoretical CNCIM calculations giving SF for the ground state smaller than for the 0^+ 6.73 MeV state and much higher SF for the first excited 2^+ than for 2^+ member of the band based on the 6.73 MeV state.

In the *sd* valence space (USDB) the third 0^+ state appears only at 11.9 MeV, and it has a relatively small alpha spectroscopic factor. Opening of the p-shell in addition to 0^+ at 6.27 MeV, leads to 0^+ state at 9.7 MeV. However, the predicted state has a low proton spectroscopic factor which is not supported by observations. A similar serious discrepancy is observed with a broad 4^{th} 2^+ state at around 9 MeV, both *sd* and *p-sd* shell models produce candidates but with very low alpha SF. As evident from our studies the only strong coupling to alpha channels could come from *fp* and higher shells. The lowest two bands saturate the alpha strength within *sd* configurations, holes in the p-shell do not lead to a significant contribution due to low level of core excitation in the ground state of ^{16}O. While our models predict high excitation energies of states with significant *fp* components, we can speculate that strong configuration mixing, collective effects such as deformation, and coupling to continuum via the super radiance mechanism [29, 30] can enhance the admixture needed to reproduce the broad resonances observed. There is a similar problem with α cluster negative parity states 1^- and 3^-, the *p-sd* Hamiltonian produces an acceptable spectrum but the alpha spectroscopic factors are low (see also Ref. [31]).

V. CONCLUSIONS

In this work we study α-clustering in ^{20}Ne. This nucleus is a benchmark example of many theoretical techniques targeting clustering in light nuclei. Our R-matrix analysis of TTIK experimental data confirms previously known results and establishes new constraints for the positions and widths of the resonances. We compared our findings with those obtained theoretically using cluster-nucleon configuration interaction approach developed in several previous works, including Ref. [2] and references therein. There is good overall agreement between theoretically predicted and observed spectra. Our theoretical approach describes very well the ground state band and the band built on the first excited 0^+ state. Allowing cross shell excitations from the p-shell, it was possible to reproduce the band built on the second 0^+ state. For these states, all spectroscopic factors for alpha transitions to the ground state of ^{16}O and to the first excited state in ^{16}O as well as proton spectroscopic factors to the ground state of ^{19}F are well reproduced. The situation is not as good when it comes to resonances 1^-, 3^- and 4^{th} 0^+ and 4^{th} 2^+, all of these states are broad and have exceptionally large alpha spectroscopic factors. In order

to describe strong clustering features these states must include configurations from *fp* shell and from higher oscillator shells. However, the Hamiltonians that we explored predict these contributions to be negligible below 15 MeV of excitation. Thus, the inability of theoretical models to describe broad states exclusively while working well elsewhere suggests an additional coupling mechanism unaccounted for in the traditional shell model Hamiltonians. The super radiance suggested in Refs. [29, 30] could provide this mechanism. Alternatively, the problem could be associated with relatively unknown cross shell interactions. Therefore, our work shows that the experimental study of alpha clustering represents an outstanding tool for exploring cross shell excitations, especially those of a multi-particle multi-hole nature.

ACKNOWLEDGMENTS

This work was supported by Ministry of Education and Science of the Republic of Kazakhstan (grant number #011503029 "NU-Berkeley", 2014-2018; grant number #0115022465, 2015-2017). This material is also based upon work supported by the U.S. Department of Energy Office of Science, Office of Nuclear Physics under Grants No DE-FG02-93ER40773 and No. DE-SC0009883. G.V.R is also grateful to the Welch Foundation (Grant No. A-1853).

[1] A. Aprahamian, K. Langanke, and M. Wiescher, Progress in Particle and Nuclear Physics **54**, 535 (2005).
[2] A. Volya and Y. M. Tchuvil'sky, Physical Review C **91**, 044319 (2015).
[3] S. Elhatisari, N. Li, A. Rokash, J. M. Alarcón, D. Du, N. Klein, B.-n. Lu, U.-G. Meißner, E. Epelbaum, H. Krebs, T. A. Lähde, D. Lee, and G. Rupak, Physical Review Letters **117**, 132501 (2016).
[4] G. R. Jansen, M. D. Schuster, A. Signoracci, G. Hagen, and P. Navrátil, Physical Review C **94**, 011301 (2016).
[5] B. A. Brown and W. A. Richter, Physical Review C **74**, 034315 (2006).
[6] D. R. Tilley, C. M. Cheves, J. H. Kelley, S. Raman, and H. R. Weller, Nuclear Physics A **636**, 249 (1998).
[7] E. Sugarbaker, R. N. Boyd, D. Elmore, and H. E. Gove, Nuclear Physics A **351**, 481 (1981).
[8] A. Arima and S. Yoshida, Physics Letters B **40**, 15 (1972).
[9] H. Cheng, H. Shen, F. Yang, and J. Tang, Nuclear Instruments and Methods in Physics Research Section B: Beam Interactions with Materials and Atoms **85**, 47 (1994).
[10] E. Berthoumieux, B. Berthier, C. Moreau, J. P. Gallien, and A. C. Raoux, Nuclear Instruments and Methods in Physics Research Section B: Beam Interactions with Materials and Atoms **136-138**, 55 (1998).
[11] H. T. Fortune, R. Middleton, and R. R. Betts, Physical Review Letters **29**, 738 (1972).
[12] H. T. Fortune, R. R. Betts, and R. Middleton, Physics Letters B **62**, 287 (1976).
[13] Y. Fujiwara, H. Horiuchi, and R. Tamagaki, Progress of Theoretical Physics **61**, 1629 (1979).
[14] L. C. McDermott, K. W. Jones, H. Smotrich, and R. E. Benenson, Physical Review **118**, 175 (1960).
[15] K. Artemov, O.P. Belyanin, A.L. Vetoshkin, R. Wolski, M.S. Golovkov, V.Z. Goldberg, M. Madeja, V.V. Pankratov, I.N. Serikov, V.A. Timofeev, Sov. J. Nucl. Phys. **52**, 408 (1990).
[16] G. V. Rogachev, E. D. Johnson, J. Mitchell, V. Z. Goldberg, K. W. Kemper, and I. Wiedenhver, AIP Conference Proceedings **1213**, 137 (2010).
[17] A. K. Nurmukhanbetova, V. Z. Goldberg, D. K. Nauruzbayev, G. V. Rogachev, M. S. Golovkov, N. A. Mynbayev, S. Artemov, A. Karakhodjaev, K. Kuterbekov, A. Rakhymzhanov, Z. Berdibek, I. Ivanov, A. Tikhonov, V. I. Zherebchevsky, S. Y. Torilov, and R. E. Tribble, Nuclear Instruments and Methods in Physics Research Section A: Accelerators, Spectrometers, Detectors and Associated Equipment **847**, 125 (2017).
[18] V. Z. Goldberg, B. T. Roeder, G. V. Rogachev, G. G. Chubarian, E. D. Johnson, C. Fu, A. A. Alharbi, M. L. Avila, A. Banu, M. McCleskey, J. P. Mitchell, E. Simmons, G. Tabacaru, L. Trache, and R. E. Tribble, Physics Letters, Section B: Nuclear, Elementary Particle and High-Energy Physics **692**, 307 (2010).
[19] N. A. Mynbayev, A. K. Nurmukhanbetova, V. Z. Gol'dberg, M. S. Golovkov, G. V. Rogachev, V. N. Dzyubin, M. V. Koloberdin, I. A. Ivanov, and R. E. Tribble, Journal of Experimental and Theoretical Physics **119**, 663 (2014).
[20] J. F. Ziegler and J. P. Biersack, in Treatise on Heavy-Ion Science: Volume 6: Astrophysics, Chemistry, and Condensed Matter, edited by D. A. Bromley (Springer US, Boston, MA, 1985), pp. 93129.
[21] E.D. Johnson, The Cluster Structure of Oxygen Isotopes, Florida State University, (2008), Ph.D. Thesis; `http://diginole.lib.fsu.edu`.
[22] J. D. Pearson and R. H. Spear, Nuclear Physics **54**, 434 (1964).
[23] Y. Utsuno and S. Chiba, Physical Review C **83**, 021301 (2011).
[24] E. K. Warburton and B. A. Brown, Physical Review C **46**, 923 (1992).
[25] E. S. Diffenderfer, L. T. Baby, D. Santiago-Gonzalez, N. Ahsan, A. Rojas, A. Volya, I. Wiedenhver, A. H. Wuosmaa, M. P. Carpenter, R. V. F. Janssens, C. J. Lister, M. Devlin, D. G. Sarantites, L. G. Sobotka, Y. Utsuno, and M. Horoi, Physical Review C **85**, 034311 (2012).
[26] S. G. Cooper, Journal of Physics G: Nuclear Physics **12**, 371 (1986).
[27] L. R. Greenwood, R. E. Segel, K. Raghunathan, M. A. Lee, H. T. Fortune, and J. R. Erskine, Physical Review C **12**, 156 (1975).
[28] R. H. Siemssen, L. L. Lee, and D. Cline, Physical Review **140**, B1258 (1965).
[29] A. Volya and V. Zelevinsky, Physics of Atomic Nuclei **77**, 969 (2014).
[30] N. Auerbach and V. Zelevinsky, Reports on Progress in Physics **74**, 106301 (2011).

[31] Y. F. Smirnov and Y. M. Tchuvil'sky, Czechoslovak Journal of Physics **33**, 1215 (1983).